

## PAWEŁ WIERZBA

Gdańsk University of Technology  
Faculty of Electronics, Telecommunication and Informatics  
Department of Optoelectronics and Electronic Systems, Poland  
e-mail: pwierzba@eti.pg.gda.pl

### STABILITY OF AN OPTICAL DISPLACEMENT SENSOR USING A TWO-BEAM POLARIZATION INTERFEROMETER

Optical interferometers can measure displacement with a resolution of tens of picometers. Polarization interferometers are often used in such measurements, as they exhibit much lower sensitivity to most of the perturbations. Although properties of these interferometers designed for metrology applications are fairly well documented, little is known about the stability of such interferometers in typical laboratory settings, where they work without vibration isolation setups or controlled flow of air. In order to assess the stability of such interferometers, a representative two-beam polarization interferometer was built on an optical plate using off-the-shelf components. Based on the results of performed measurements it is possible to conclude that such interferometers can be used for measurements when a drift of the order of ten nanometers during a 30 s interval is acceptable.

Keywords: polarization interferometry, two-beam interferometer, displacement measurement, stability of interferometers

#### 1. INTRODUCTION

Optical interferometry is one of the most sensitive and most accurate measurement techniques. Interferometric displacement sensors capable of attaining picometer resolution have been demonstrated (e.g. [5]) and have found widespread use in several fields of science and engineering.

A classic displacement sensor using a Michelson interferometer is presented in Fig. 1. Light from a monochromatic light source LS is incident on the non-polarizing beam splitter BS, which divides it into measurement and reference beams that usually have equal intensities. The reference beam, which propagates in the reference arm, is reflected from fixed mirror M1, while the measurement beam, propagating in the measurement arm, is reflected from movable mirror M2 attached to the object whose displacement is to be measured. Both beams return to the BS which combines them and divides the combined beam into a beam returning to the light source and a beam incident on a detector D, usually a photodiode.

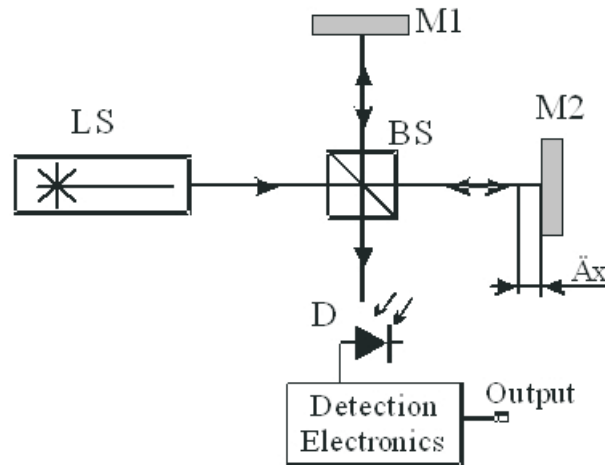


Fig. 1. Michelson interferometer.

Assuming that the components do not introduce any loss, the states of polarization of both beams are identical and that both beams have equal intensities, light intensity  $I$  at the detector D can be expressed as:

$$I(\Delta x) = \frac{I_0}{2} \left[ 1 + \cos \left( \frac{2\pi}{\lambda} 2n\Delta x \right) \right], \quad (1)$$

where  $I_0$  – light intensity at the output of the source,  $n$  – refractive index of air,  $\Delta x$  – measured displacement,  $\lambda$  – wavelength of the source. Detector D produces an electrical signal proportional to the light intensity  $I$ ; this signal is processed by the electronic circuit which produces an output voltage signal whose value is proportional to  $I$ .

An important problem encountered in interferometric measurement is instability of the states of polarization of interfering beams arising from uncontrolled fluctuations of polarization properties of optical components (e.g. lenses, beam splitters) comprising the interferometer. As a result, the light intensity  $I$  at detector D becomes:

$$I(\Delta x) = \frac{I_0}{2} \left[ 1 + V \cos \left( \frac{2\pi}{\lambda} 2n\Delta x \right) \right], \quad (2)$$

where  $V$  – interference contrast, also known as fringe visibility. Because  $I$  no longer depends only on  $\Delta x$  and the value of  $V$  at a given point of time is unknown due to the random nature of the aforementioned fluctuations,  $\Delta x$  cannot be accurately determined from  $I$ .

A solution which substantially mitigates the influence of these fluctuations on accuracy of the measurement is the use of polarization interferometers, in which birefringent components, such as polarizing beam splitters or Wollaston prisms, are used in order

to obtain stable states of polarizations of beams propagating in these interferometers. While the performance of polarization interferometers can be degraded by phenomena such as polarization mixing or parasitic reflections (cf. e.g. [4, 9]), with adequate care it is possible to attain measurement resolution in the picometer range.

Polarization interferometers that reach such resolution are sensitive to several environmental perturbations, such as vibration, air currents and temperature fluctuations. When used in metrology applications, where ultimate accuracy is sought, these interferometers can be built on vibration isolation platforms and operated in a controlled atmosphere or even in an evacuated environment.

However, often it is desirable to use custom-built polarization interferometers to monitor displacement in experiments conducted outside the confines of optical metrology laboratories, i.e. without elaborate protection against environmental perturbations. Before attempting to do so, it is worthwhile to determine how polarization interferometers would perform. Stability of such interferometer is usually the crucial factor, especially when the duration of the measurement becomes comparable to the period of fluctuations.

Since investigation of all known types of polarization interferometers would be a massive undertaking, given the number of known interferometers, a representative example of a polarization interferometer was chosen for further investigation.

In order to investigate the performance of this interferometer in the worst-case scenario, optical path lengths in both arms were made unequal, which increased the sensitivity of the interferometer to fluctuations in the wavelength of the source illuminating it. Moreover, a detection setup used in the interferometer is also sensitive to fluctuations of the output power of the source illuminating the interferometer.

The primary objective of this paper is to investigate the stability of a representative two-beam polarization interferometer used for measurement of displacement. Section 2 gives a brief description of two polarization interferometers used for measurement of displacement. The measurement setup is described in Section 3, while measurement results are presented in Section 4 and discussed in Section 5. Finally, conclusions and directions of further research are presented in Section 6.

## 2. POLARIZATION INTERFEROMETERS

Most polarization interferometers are two-beam interferometers, although multiple-beam interferometers were also demonstrated [1]. Polarization interferometers are implemented either as modifications of existing interferometers (e.g. Michelson interferometer) or as setups designed specially for polarization interferometry.

An example of a polarization interferometer belonging to the latter class is an interferometer proposed by Dyson in [2] and presented in Fig. 2a. Light from a source LS, polarized circularly or linearly at  $45^\circ$  to the plane of Figure is incident on a Wollaston prism WP, which divides it into the reference beam (solid line) polarized

perpendicularly to the plane of the Figure and the measurement beam (dashed line) polarized in the plane of the Figure. Both beams propagate through a lens L, are reflected from surfaces M3 and M2, respectively and propagate again through the lens L. Subsequently, they are transmitted through a quarter-wave plate QWP, whose fast axis is aligned at  $45^\circ$  to the plane of the Figure, are reflected from a mirror M1 and return through the quarter-wave plate QWP. Upon propagating twice through the quarter-wave plate QWP the measurement beam becomes polarized perpendicularly to the plane of the Figure, while the reference beam becomes polarized in the plane of the Figure. Both beams are transmitted through the lens L, reflected from surfaces M2 and M3' respectively. Subsequently they return, through the lens L, to the Wollaston prism WP, which combines them into one beam whose state of polarization is a function of the phase difference introduced by the measured displacement  $\Delta x$ . Detection setup DS produces an electrical signal corresponding to the state of polarization of that beam, from which the measured displacement  $\Delta x$  can be inferred.

The sensitivity of this interferometer is twice as high as that of the Michelson interferometer, as the measured displacement  $\Delta x$  gives rise to the change of optical path difference of  $4\Delta x$ , while in the Michelson interferometer the change of optical path difference is  $2\Delta x$ . As a result Eq. (2) for this interferometer becomes

$$I(\Delta x) = \frac{I_0}{2} \left[ 1 + V \cos \left( \frac{2\pi}{\lambda} 4n\Delta x \right) \right]. \quad (3)$$

However, this interferometer is difficult to align, mostly due to closely spaced WP, M1 and QWP. Moreover, the angle  $\alpha$  between the input and the output beam is usually small ( $\alpha < 20^\circ$ ) hampering the alignment of the optical part with the light source LS and detection setup DS. The angle  $\alpha$  cannot be easily increased since it depends on the splitting angle of the Wollaston prism which in turn is limited by birefringence of available materials.

In order to address these shortcomings while retaining the sensitivity, a polarization interferometer presented in Fig. 2b was devised by Roberts [6, 7]. Its operation is similar to that of the previously described interferometer. Light beam  $w_I$ , linearly polarized perpendicularly to the plane of the Figure is reflected by mirror M1 and falls on a double-side non-polarizing beam splitter DNBS – a glass plate with semi-reflective coating applied on each surface. Reference beam  $w_R$  (solid line) and measurement beam  $w_M$  (dashed line) are created from the input beam  $w_I$  in the non-polarizing beam splitter DNBS. They subsequently propagate in the interferometer, in a way similar to that described previously. When the reference beam  $w_R$  and measurement beam  $w_M$  return to the non-polarizing beam splitter DNBS, they are both polarized in the plane of the Figure. A half-wave plate whose fast axis is aligned at  $45^\circ$  to the plane of the Figure rotates the plane of polarization of the reference beam  $w_R$  by  $90^\circ$  – the reference beam becomes polarized perpendicularly to the plane of the Figure. Subsequently, both

beams are combined by the non-polarizing beam splitter DNBS into the output beam  $w_O$ , which propagates to the detection setup DS.

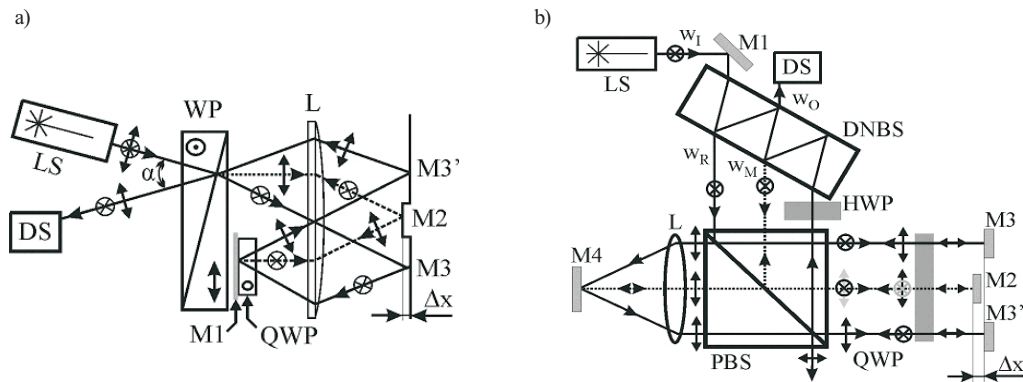


Fig. 2. Polarization interferometer designed by Dyson [2]. (a), Interferometer designed by Roberts [7] as a modification of interferometer from Fig. 2a.

The interferometer from Fig. 2b is much easier to align. The reference beam  $w_R$  and measurement beam  $w_M$  propagate always in close proximity, which should improve the immunity of the interferometer to the flow of air and to vibrations. Moreover, the spacing of the beams can be controlled by choosing a the non-polarizing beam splitter DNBS of suitable thickness (or by making it from two plate beam splitters whose spacing is varied). Taking into account the advantages of this interferometer, it was selected as the basis for the measurement setup described in the following Section.

### 3. MEASUREMENT SETUP

Upon a more detailed analysis of operation of the interferometer presented in Fig. 2b, it was concluded that a further modification is possible, in which *reflected* (rather than *transmitted*) components of the reference beam  $w_R$  and measurement beam  $w_M$  are combined into the output beam  $w_O$ , as shown in Fig. 3a. As a result the separation between the input and the output beam is greatly increased, thereby facilitating setting up of the interferometer. Mirror M1 is not necessary and was used for convenience reasons.

The interferometer presented in Fig. 3a was built from off-the-shelf optical and mechanical components on an optical breadboard. A helium-neon laser operating at  $\lambda = 632.8$  nm with an MC1000 chopper, made by Thorlabs Inc, operating at 108 Hz was used as the light source LS. The detection setup DS was implemented using a polarizer followed by a silicon photodiode connected to a Newport 840 optical power meter. The signal from the optical power meter was fed to the input of an Ithaco 3961B lock-in amplifier, whose reference input was driven by the reference signal from the

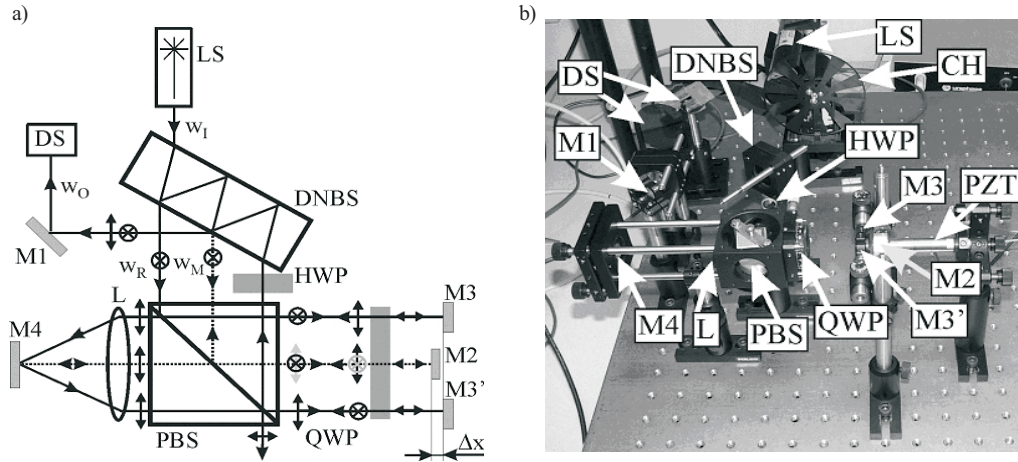


Fig. 3. Modified interferometer from Fig. 2b. a) layout, b) view of the setup. CH – chopper, PZT – piezoelectric actuator.

chopper controller. Data acquisition was performed by an SR785 Dynamic Signal Analyser, made by Stanford Research Systems. Mirror M2 was attached to the tip of a P-841.20 piezoelectric actuator PZT, controlled by an E655XR digital controller, both produced by Physik Instrumente GmbH. This provided a convenient way of adjusting the operating point of the interferometer. Stability of the position of the actuator is better than 1nm, according to the manufacturer data.

The optical path length in the reference arm of the interferometer was  $655 \pm 5$ mm. Such a high uncertainty stems from the difficulty in measuring distances between certain optical components without disturbing their alignment. Particularly troublesome were measurements of the distances between the polarizing beam splitter PBS and the non-polarizing beam splitter DNBS, as well as between the PBS and mirrors M2, M3, M3'. Optical path length in the measurement arm of the interferometer was longer by  $\Delta l = 48 \pm 1$ mm than that in the reference arm. This length difference was introduced in order to operate this interferometer in the worst case scenario, in which optical path lengths in both arms cannot be made equal. In such a case the light intensity  $I$  at detector D given by (3) becomes

$$I(\Delta x) = \frac{I_0}{2} \left[ 1 + V \cos \left( \frac{2\pi}{\lambda} n (4\Delta x + \Delta l) \right) \right]. \quad (4)$$

The interferometer becomes more sensitive to the fluctuations of the laser wavelength, as we shall see in Section 5.

#### 4. MEASUREMENT RESULTS

The measurement setup described in the previous section was built and tested by generating a linear displacement sweep lasting 40 s. The response of the measurement setup was recorded and compared with the theoretical dependence – Eq. (4). No significant distortion was found in the response, indicating that the interferometer was essentially free from nonlinearity sources. Interference contrast  $V$  was equal to 0.725, due to slight depolarization of the interfering beams and lack of complete overlap of both beams, apparently caused by aberrations of used lens L.

Subsequently a measurement of interferometer drift was performed. The interferometer was set up to operate at maximum sensitivity. Data acquisition was set up for an acquisition period of 32 s and several measurements were subsequently performed. The recorded voltage signal  $u(t)$  was proportional to the intensity  $I$  of light from the interferometer incident on the detector D. Measured displacement drift  $\Delta x(t)$  was calculated using (4) from the acquired signal  $u(t)$ . An exemplary measurement result, showing an average amount of drift, is presented in Fig. 4. In a few cases the measurement was disrupted by transients whose amplitude was at least an order of magnitude greater than that of the acquired signal. Although the exact nature of these transients is unknown, it is supposed that they were caused either by wireless transmitting equipment (mobile phones, wireless network infrastructure) or resulted from office equipment or electric power tools.

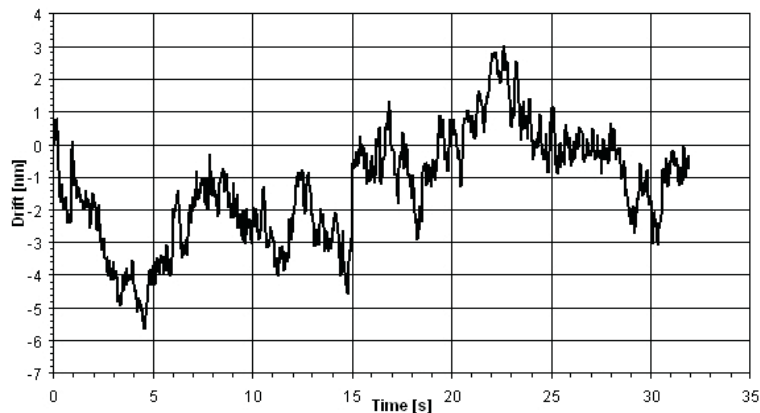


Fig. 4. Measured drift of the interferometer from Fig. 3.

#### 5. DISCUSSION

The data presented in Fig. 4 confirm good stability of the tested interferometer. The peak-to-peak value of the drift is below 9nm. In most measurements the peak-to-peak

value of the drift is below 12nm. This stability is acceptable in a broad range of applications.

Apart from environmental perturbations, this drift can be caused also by fluctuations in the wavelength and output power of the laser. In most cases it is stipulated that these fluctuations are not the dominant cause of the drift. Therefore, let us consider the conditions on the wavelength and output power stability that result from this requirement. For further analysis we assume that the drift  $x$  caused by each of these factors does not exceed 1nm. Differentiating (4) with respect to  $x$  at the operating point of the interferometer we arrive at:

$$\frac{\partial I}{\partial(\Delta x)} = \frac{4\pi V n I_0}{\lambda}. \quad (5)$$

Therefore, stability of intensity that results in drift  $\delta x$  is given by:

$$\frac{\Delta I}{I} = \frac{8\pi V n}{\lambda} \delta x. \quad (6)$$

In our case the intensity of the laser must be stable to within 2.9%. When a laser having adequate output power stability cannot be used, it is still possible to reduce the drift resulting from instability of the output power by using detection setups with source intensity noise cancellation, such as those described in [3] or in [8].

The required stability of wavelength can be calculated using a similar method. For the discussed interferometer the emitted wavelength must be stable to within 0.05 pm. If the optical path difference between the arms of the interferometer can be reduced, the requirement on the stability of emitted wavelength can be relaxed. A good example of application where the optical path difference can be close to zero is pressure measurement using the presented interferometer, discussed e.g. in [10].

## 6. CONCLUSIONS

The polarization interferometer investigated in this paper offers good stability without resorting to vibration isolation and air flow control. The peak-to-peak value of the drift during a 32 s measurement period in most measurements is below 12 nm. This stability can be attained when a laser is used whose wavelength stability is better than 0.05 pm and output power is stable to within 2.9%. The requirement on the stability of the output power can be further relaxed by using detection setups with source intensity noise cancellation. If optical paths in both arms of the interferometer can be made equal, also the requirement on the stability of the wavelength can be substantially relaxed, allowing inexpensive DFB lasers to be used as the light source illuminating the interferometer.



## ACKNOWLEDGEMENTS

Partial support of this research by project of MNiI no 4 T11B 032 26 is thereby gratefully acknowledged, as is the support from DS and BW allocations of the ETI Faculty of the Gdansk University of Technology.

## REFERENCES

1. Chauvat D., et. al.: "Jamin Fabry – Perot interferometer", *Optics Letters*, vol. 28, no. 2, 2003, pp. 126–128.
2. Dyson J.: "Optics in a hostile environment", *Applied Optics*, vol. 7, 1968, pp. 569–580.
3. Hobbs P. C. D.: "Ultrasensitive laser measurements without tears", *Applied Optics*, vol. 36, no. 4, 1997, pp. 903–920.
4. Heydemann P. L. M.: "Determination and correction of quadrature fringe measurement errors in interferometers", *Applied Optics*, vol. 20, no. 19, 1981, pp. 3382–3384.
5. Lawall J., Kessler E.: "Michelson interferometry with 10 pm accuracy", *Review of Scientific Instruments*, vol. 71, no. 7, 2000, pp. 2669–2676.
6. Roberts R. B.: "Absolute dilatometry using a polarization interferometer", *Journal of Physics E: Scientific Instrumentation*, vol. 8, 1974, pp. 600–602.
7. Roberts R. B.: "Absolute dilatometry using a polarization interferometer: II", *Journal of Physics E: Scientific Instrumentation*, vol. 14, 1981, pp. 1386–1388.
8. Stamm C., Lukosz W.: "Integrated optical difference interferometer as refractometer and chemical sensor", *Sensors and Actuators B*, vol. 11, 1993, pp. 177–181.
9. Wierzba P., Kosmowski B. B.: "Accuracy Improvement of bulk optical polarization interferometric sensors", *Optica Applicata*, vol. 35, no. 1, 2005, pp. 171–185.
10. Wierzba P.: "Modeling of selected transducer designs for optical pressure sensors using polarization interferometry", *Proc. of the SPIE*, vol. 6348, 2006, pp. 634802–1 - 634802–7.